

# Noninvasive Assessments of Optic Nerve Neurodegeneration in Transgenic Mice With Isolated Optic Neuritis

Venu Talla,<sup>1</sup> Cui Yang,<sup>2</sup> Gerry Shaw,<sup>2,3</sup> Vittorio Porciatti,<sup>1</sup> Rajeshwari D. Koilkonda,<sup>1</sup> and John Guy<sup>1</sup>

<sup>1</sup>Bascom Palmer Eye Institute, University of Miami Miller School of Medicine, Miami, Florida

<sup>2</sup>Department of Neuroscience, University of Florida College of Medicine, Gainesville, Florida

<sup>3</sup>EnCor Biotechnology Inc., Gainesville, Florida

Correspondence: John Guy, Bascom Palmer Eye Institute, McKnight Vision Research Center, 1638 NW 10th Avenue, Miami, FL 32610; jguy@med.miami.edu.

Submitted: February 19, 2013

Accepted: May 22, 2013

Citation: Talla V, Yang C, Shaw G, Porciatti V, Koilkonda RD, Guy J. Noninvasive assessments of optic nerve neurodegeneration in transgenic mice with isolated optic neuritis. *Invest Ophthalmol Vis Sci*. 2013;54:4440–4450. DOI:10.1167/iops.13-11899

**PURPOSE.** To determine if phosphorylated neurofilament heavy chain (pNF-H) released into the bloodstream and the pattern ERG are noninvasive indicators of neurodegeneration in experimental optic neuritis.

**METHODS.** Serum from Myelin oligodendrocyte glycoprotein (MOG)-specific T cell receptor-positive (TCR+) transgenic mice that develop isolated optic neuritis usually without any other characteristic lesions of inflammation or demyelination in the spinal cord and littermates negative for the transgene were assayed for the presence of serum phosphorylated neurofilament H (pNF-H). In vivo measurements of optic nerve and retinal ganglion cell injury were assessed by magnetic resonance imaging (MRI), optical coherence tomography (OCT), and pattern electroretinogram (PERG). Automated two dimensional fluorescence differential in-gel electrophoresis (2D-DIGE) of pooled optic nerve samples, light, and transmission electron micrographs were used to evaluate optic atrophy postmortem.

**RESULTS.** We found an almost 3-fold elevation in serum pNF-H levels in MOG+ mice relative to MOG-littermates ( $P = 0.02$ ). 2D-DIGE revealed a 3-fold reduction in optic nerve neurofilaments. Visual function assessed by the PERG was reduced by one-quarter ( $P = 0.033$ ) and latencies increased by 38% ( $P = 0.036$ ). MOG+ mice with the lowest PERG amplitudes had optic nerve atrophy visualized by MRI. Optic nerve diameters were reduced by one-third ( $P = 0.0001$ ) and axon counts reduced by more than two-thirds. Histopathology of the spinal cords was normal.

**CONCLUSIONS.** Elevated serum pNF-H levels and the PERG are useful markers of neurodegeneration of the optic nerve in isolated experimental optic neuritis. Our findings suggest that elevations of this axonal protein in patients with optic neuritis who had a poor visual outcome are likely also due to demise of optic nerve axons.

**Keywords:** optic neuritis, neuroophthalmology, neurodegeneration, axonal degeneration, neurofilaments

Axonal and neuronal loss is increasingly recognized as the cause of persistent deficits and disability in optic neuritis and multiple sclerosis (MS).<sup>1–4</sup> Petzold and colleagues have described elevated levels of serum or plasma phosphorylated neurofilament heavy chain (pNF-H) in optic neuritis associated with multiple sclerosis or neuromyelitis optica (NMO) that correlated with poor recovery of visual function<sup>5</sup> and later conversion to multiple sclerosis.<sup>6,7</sup> We found increased serum pNF-H levels in optic neuritis patients who had severe baseline visual deficits.<sup>8</sup> OCT detected the late retinal nerve fiber loss after the axons had died off, but it is not useful initially for selecting at initial presentation the 8.5% of optic neuritis patients who are left with 20/40 or worse.<sup>9</sup> Such patients may benefit from neuroprotection to prevent irreversible optic neuropathy and permanent visual loss.

Axons contain neurofilaments that are the major component of the axonal cytoskeleton. Neurofilaments are structural proteins consisting of at least three major subunits—the light,

medium and heavy chains (NF-L, NF-M, and NF-H)—which may be released into the bloodstream following axonal disruption. The heavily phosphorylated axonal form of NF-H, pNF-H, has a collection of unusual properties that render it resistant to proteases and relatively easy to detect with ELISA and other antibody-based assays.<sup>10,11</sup> Thus, serum pNF-H levels provide a prospective measure of neurodegeneration. What is unclear from previous studies is whether the optic nerve, brain, or spinal cord was the source of neurofilaments detected in the systemic circulation.

Retinal ganglion cell (RGC) and axonal loss are also evident in the most frequently utilized animal model of MS, experimental autoimmune encephalomyelitis (EAE).<sup>12–15</sup> Elevations in serum pNF-H have been detected in animals with the characteristic paralysis of EAE, but this is due to involvement of the spinal cord and not the optic nerve.<sup>16</sup> As verification that axonal loss from optic neuritis can also be a source of the pNF-H in patients with optic neuritis, we turned to transgenic TCR

MOG+ mice that develop isolated optic neuritis.<sup>17</sup> In this report, we show elevated serum pNF-H levels in transgenic mice that have isolated optic neuritis<sup>18</sup> with histopathologic confirmation that axons are lost predominantly in the optic nerve and not in the spinal cord. Thus, serum pNF-H elevations in these mice corroborate our suggestion that the elevated level of this biomarker in optic neuritis and MS patients is due to axonal injury of the optic nerve.

## MATERIALS AND METHODS

### Experimental Animals

MOG-specific TCR transgenic mice that develop isolated optic neuritis usually without any other characteristic lesions of EAE in the brain or in the spinal cord were a gift of Vijay Kuchroo.<sup>18</sup> Littermates negative for the transgene or age-matched normal C57BL6 mice served as controls. To increase the incidence of optic neuritis, animals received intraperitoneal pertussis toxin.<sup>17</sup> Mice were examined 4 to 6 months after birth.

### pNF-H Assay

Serum from 14 TCR MOG+ mice and 14 littermates negative for the transgene were assayed for the presence of pNF-H as previously described, using an assay identical to the pNF-H ELISA obtainable commercially from EnCor Biotechnology Inc. (Gainesville, FL).<sup>8,19,20</sup>

### Two-Dimensional Fluorescence Differential In-Gel Electrophoresis (2D-DIGE)

2D-DIGE was performed on the total protein from the optic nerves of the transgenic MOG+ and C57BL6 mice. The procedure followed was the same as reported by Lehmsiek et al.<sup>21</sup> Briefly, 50 µg protein from the MOG+, C57BL6, and an internal standard (1:1 ratio of MOG+ and C57BL6) were dissolved in a small volume of labeling buffer (8 M Urea, 4% CHAPS, and 30 mM Tris/HCl pH 8.5) and labeled with three different N-hydroxysuccinamide cyanine dyes (CyDyes; Amersham Biosciences, Little Chalfont, Buckinghamshire, UK). The internal standard was labeled with Cy2, MOG+ labeled with Cy3, and that of C57BL6 was labeled with Cy5. Each of these labeling CyDyes were reconstituted in anhydrous dimethyl formamide (DMF) and mixed with samples at a ratio of 400 pmole CyDye per 50 µg protein and incubated on ice for 30 minutes. The reaction was stopped by adding 2.8 µL of 10 mM lysine for 15 minutes on ice. The proteins were resolved by isoelectric focusing (IEF) followed by SDS-PAGE using methods used by Lehmsiek et al.<sup>21</sup> After electrophoresis, gels were fixed in 30% ethanol and 10% acetic acid for 1 hour and then transferred into 1% acetic acid. Gels were scanned with Typhoon 9400 imager (GE Healthcare Biosciences, Pittsburgh, PA) at excitation/emission values of 488/520 nm for Cy2 dye, 532/580 nm for Cy3 dye, 633/670 nm for Cy5 dye. Data analysis software (DeCyder software, version 6.0; Amersham Biosciences) codetected and differentially quantified the protein spots in the images after matching, quantitation, and statistical analysis between the two gels (MOG+ and MOG-) and directly provided the ratio of spot density of MOG+ to controls.

### ERG Recordings

Pattern ERGs obtained for eight transgenic MOG+ mice and six normal C57BL6 mice were performed as previously described.<sup>22,23</sup> Briefly, a visual stimulus of contrast-reversing bars (field area, 50° × 58°; mean luminance, 50 cd/m<sup>2</sup>; spatial

frequency, 0.05 cyc/deg; contrast, 100%; temporal frequency, 1 Hz) was aligned with the projection of the pupil at a distance of 20 cm. The retinal signals were amplified by 10,000-fold and bandpass filtered by 1 to 30 Hz. Three consecutive responses to each of the 600 contrast reversals were recorded, checked for their consistency by superimposition, and were averaged.<sup>24</sup> Averaged pattern electroretinogram (PERG) waveforms were analyzed to evaluate the major positive and negative waves using commercially available software (Sigma Plot; Systat Software Inc., San Jose, CA). To prevent bias in evaluation of peaks and troughs of PERG waveforms with reduced amplitude, we calculated the root-mean-square (RMS) voltage of the PERG signal. Response amplitude was defined as the RMS voltage over a time epoch of 0 to 350 ms after each contrast reversal according to the equation ( $VRMS = \sqrt{[\sum v_i^2]/n}$ ), where VRMS is the amplitude,  $v_i$  is the voltage at each sampled time point, and  $n$  is the number of sampled points. RMS evaluation was automatically performed using a macro written in statistical language (SigmaPlot 11.2; Systat Software Inc.). Statistical analysis was performed by Student's *t*-test for unpaired data.  $P < 0.05$  was considered statistically significant.

### Spectral-Domain Optical Coherence Tomography (SD-OCT) Imaging in Live Mice

In vivo high-resolution three-dimensional (3D) imaging of the live mouse retina was performed using SD-OCT (Bioptigen, Inc., Durham, NC), as described previously.<sup>25</sup> Briefly, the mice were anesthetized with an intraperitoneal injection of ketamine (80 mg/kg) and xylazine (5 mg/kg). Pupils were dilated with a drop of 1% tropicamide and lubricating eye drops (Systane Ultra; Alcon Laboratories, Inc., Fort Worth, TX) were applied to preserve the corneal hydration and to increase the clarity. The mice were restrained on a custom stage that was fixed on a six-axis platform, which allowed free rotation, to align the eye for imaging of the optic nerve head (ONH). Raster scans—typically measuring 512 × 128 (horizontal × vertical) and 1024 × 64 depth scan patterns, with the fast scan in the horizontal direction, were performed for each eye. Scan length was approximately 32° for imaging mouse retinas. The images obtained from the MOG+ and control C57BL6J mice were observed for structural changes at the optic nerve head, the nerve fiber, and RGC layer.

### Magnetic Resonance Imaging (MRI) of the Optic Nerves in Live Mice

High-resolution three-dimensional MRI of MOG+ and normal C57BL6 mice was performed as reported earlier.<sup>26,27</sup> The animals were kept under isoflurane 1.5% to 2% anesthesia. All animals were placed in a prone position with their heads firmly fixed in a purpose built surface coil. MR imaging was performed before and after intraperitoneal administration of contrast. Three-dimensional images were acquired with a 4.7 Tesla small-bore magnet (Oxford Instruments, Oxford, UK).

### Light and Electron Microscopy

MOG+ mice and littermates negative for the transgene were euthanized with sodium pentobarbital. They were then perfused by cardiac puncture with fixative consisting of 4% paraformaldehyde in 0.1 M PBS buffer (pH 7.4). The eyes with attached optic nerves were dissected out and further processed by immersion in 2.5% glutaraldehyde, postfixed in 1% osmium tetroxide, 0.1 M sodium cacodylate-HCl buffer (pH 7.4), 7% sucrose in the cold, and then dehydrated through an ethanol series to propylene oxide, infiltrated, and embedded in epoxy resin and polymerized at 60°C overnight. Semithin

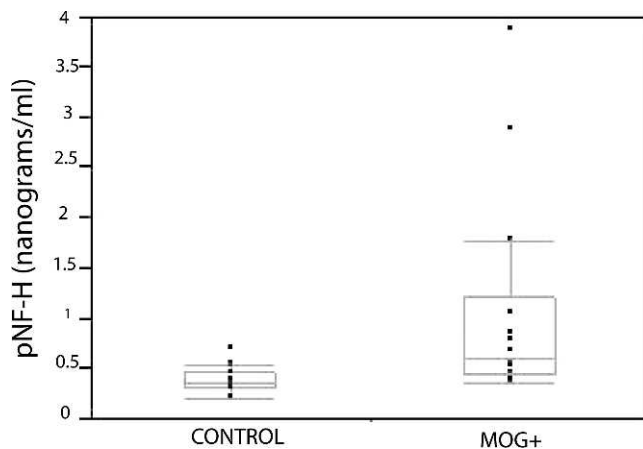


**FIGURE 1.** Serum pNF-H Quantitation. A scatterplot with quantile boxes of serum pNF-H levels of individual animals shows that the highest value in controls was 0.7 ng/mL. Six affected animals had pNF-H values greater than 0.7 ng/mL. The lowest line of the quantile plot represents the 10th percentile and the highest line the 90th percentile. The *bottom* of the quantile box represents the 25th percentile and the *top* of the box the 75th percentile, with the median value in the *middle* of the box. Median values are slightly different than the means.

longitudinal sections (0.5  $\mu$ m) of the globe and optic nerve were stained with toluidine blue for light microscopic examination. Optic nerve diameters were quantitated by a masked observer as previously described.<sup>27</sup> Ultrathin sections (90 nm) were placed on copper mesh grids for examination with a Hitachi H-7600 transmission electron microscope (Hitachi Inc., Tokyo, Japan) operating at 80 kV. Optic nerve axons were counted by a masked observer as previously described.<sup>23</sup>

### Statistical Analysis

Statistical analysis of differences in serum pNF-H levels, PERG amplitude, latency of transgenic MOG+, and control mice were performed by Student's *t*-test for unpaired data. *P* values of 0.05 or less were considered significant.

## RESULTS

### Serum pNF-H Levels Are Elevated in Transgenic MOG+ Mice

Indicative of neurodegeneration, we found an almost 3-fold elevation in serum pNF-H levels in MOG-specific TCR transgenic mice relative to control littermates. Mean serum pNF-H for the MOG-specific TCR transgenic mice was  $1.07 \pm 0.28$  (mean  $\pm$  SEM) nanograms per milliliter (ng/mL) relative to a mean value of  $0.38 \pm 0.03$  ng/mL for the control littermates. This difference was statistically significant ( $P = 0.02$ ). A scatter plot shows that levels of pNF-H were markedly elevated, greater than 1 ng/mL, in four MOG+ TCR transgenic mice (Fig. 1). However, none of the littermates had levels greater than 0.70 ng/mL. If pNF-H is released into the bloodstream from damage to optic nerve axons then neurofilament levels in the optic nerve should be reduced.

### Neurofilament Levels Are Reduced in the Optic Nerves of Transgenic MOG+ Mice

Indeed, automated 2D-DIGE of the pooled optic nerve samples from both eyes of 20 MOG+ mice revealed a 3-fold reduction in neurofilament levels (Fig. 2A) relative to an equal number of

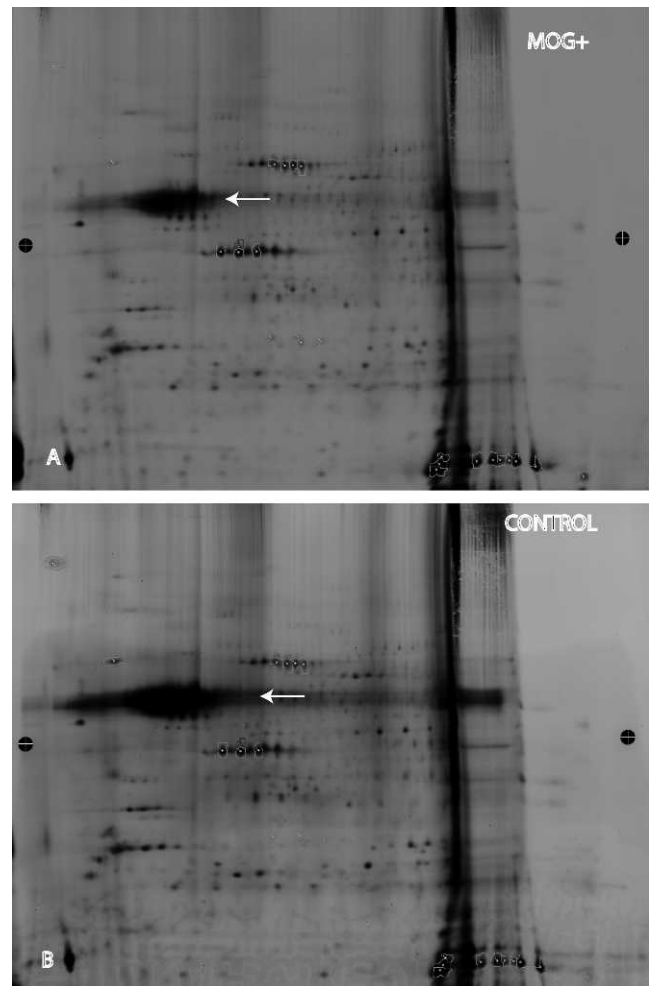


**FIGURE 2.** Optic nerve neurofilament protein analysis. (A) 2D-DIGE of optic nerve protein samples from transgenic MOG+ mice showed the neurofilament heavy chain protein band (*arrow*) was one of the largest bands on the gel. (B) The neurofilament heavy chain band (*arrow*) of nontransgenic control mice was much larger than that of MOG+ mice.

control littermates that were negative for the transgene (Fig. 2B). Even with this reduction, the neurofilament band was still the largest of any optic nerve protein on the gel. Thus, the source of pNF-H elevations in serum appeared to be due to loss of neurofilaments in the optic nerve.

### Visual Function Is Reduced in MOG+ Mice

Next, we wondered whether such profound loss of neurofilaments in the optic nerve had any measurable effect on visual function in the mouse. Using the pattern electroretinogram (PERG) as a sensitive measure of retinal ganglion cell function, we performed PERGs on eight transgenic MOG+ mice with comparisons to six normal animals. Signals from the right and left eyes were averaged to give a mean value for each animal. We found the root-mean-square (RMS) voltage of the PERG signal of MOG+ mice of  $4.45 \pm 1.79$   $\mu$ V (mean  $\pm$  SD) was reduced 26% relative to MOG- mice with a value of  $6.05 \pm 1.93$   $\mu$ V. In addition, the PERG latency was prolonged by 38% in transgenic mice ( $122 \pm 32$  ms), relative to controls ( $88 \pm 5$  ms),  $P = 0.036$ . The PERG RMS (Fig. 3A), amplitudes (Fig. 3B), and latencies (Fig. 3C) for individual right and left eyes of MOG+ and MOG- mice were plotted. The PERG waveforms shown illustrate the loss of amplitude and increase in latency of

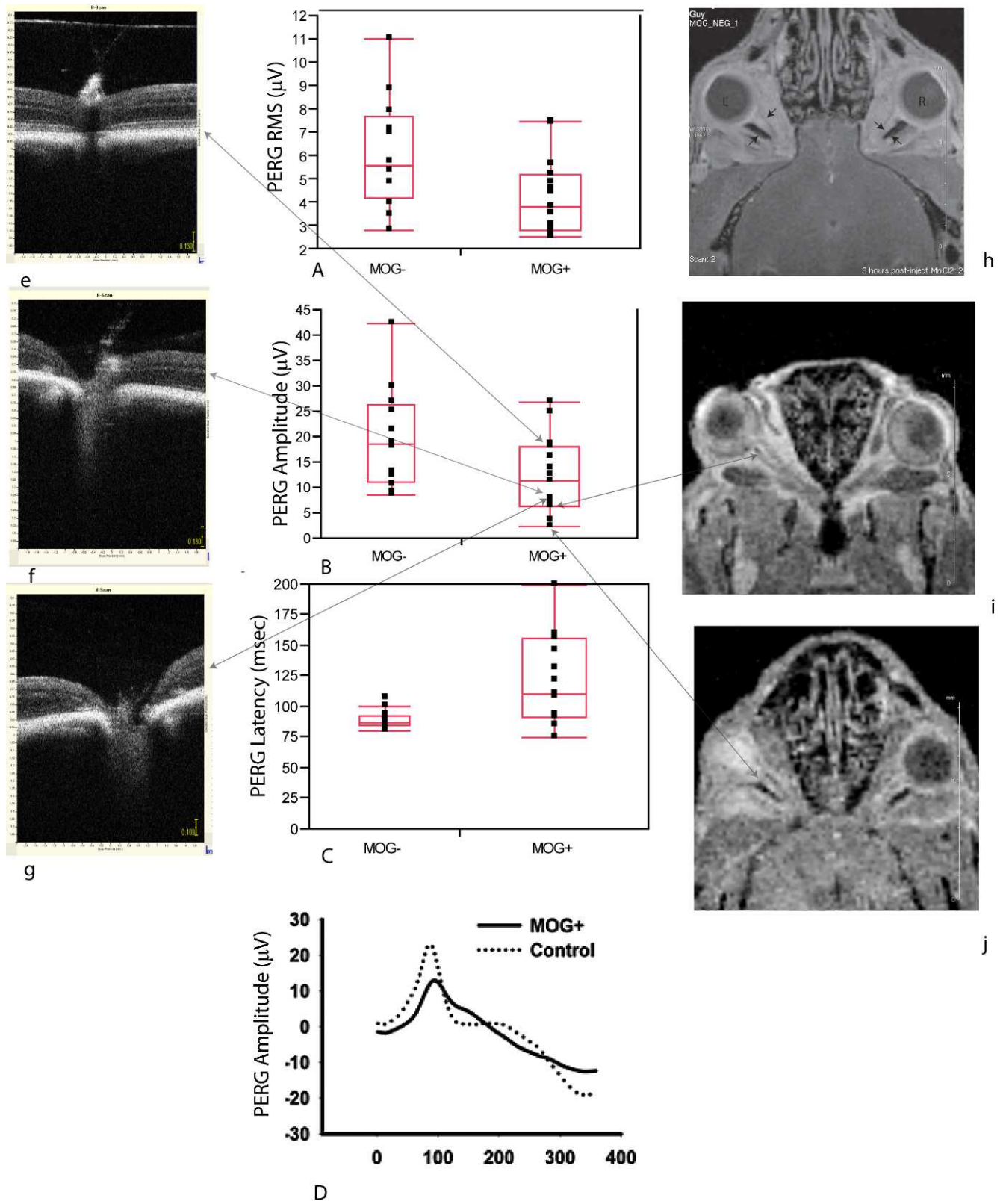


**FIGURE 3.** Electrophysiology of visual function, SD-OCT, and MRI. (A) Scatter plots of values for individual eyes with quantile boxes show PERG RMS (A), PERG amplitudes (B), and PERG latencies of MOG+ mice compared with controls (C). Representative PERG waveforms of MOG+ and control mice illustrate both the loss in amplitude and delay of the signal (D). The large arrows connect the PERG amplitude of three MOG+ eyes to the OCT images (e-g) and two MOG+ eyes to the MRI images (h, i). Small arrows point to the optic nerve on the MRI images. L, left eye; R, right eye.

experimental relative to control animals (Fig. 3D). As alterations in the PERG are consistent with visual loss due to dysfunction and/or loss of retinal ganglion cells in transgenic MOG+ mice with optic neuritis, our next step was to determine whether changes in the PERGs reflected loss of function and/or structure.

### Optic Nerve Atrophy Visualized by SD-OCT and MRI in Transgenic MOG+ Mice

To examine structure, we used two noninvasive imaging modalities commonly used in patients with optic neuritis and MS. First, we used high-resolution SD-OCT. In an MOG+ mouse that had a good PERG amplitude, OCT cross-sectional imaging of the optic nerve head appeared normal (Fig. 3e). However, in two MOG+ mice with extremely low PERG signals, the optic nerve head appeared excavated (Figs. 3f, 3g). Unfortunately, the RGC layer of the mouse could not be resolved by OCT. We also evaluated the optic nerve using MRI. The retrobulbar left optic nerves of two MOG+ mice were much thinner than the right optic nerves (Figs. 3h, 3i). The PERG signal from these two eyes had extremely low amplitudes. MR imaging revealed no brain lesions that could if present contribute to axonal loss causing elevated neurofilament heavy chain levels in serum.

### Atrophy of the MOG+ Optic Nerve

Lastly, we used histopathology as the gold standard for assessing optic atrophy and axonal loss. Longitudinal sections of the retrobulbar optic nerve counterstained with toluidine blue show the normal nerve of littermates without the transgene (Fig. 4A). In contrast, the retrobulbar optic nerve of transgenic MOG+ mice showed moderate (Fig. 4B) to severe optic atrophy (Fig. 4C) without excavation of the optic nerve head. Foci of demyelination were present in the retrobulbar optic nerve (Figs. 4D, 4E). At higher magnification, normal myelinated axons were evident in MOG- littermates (Fig. 4F). The characteristic inflammatory demyelinating lesion was evident in optic nerves of transgenic MOG+ mice (Fig. 4G). Optic nerve diameters of MOG+ mice were reduced by one-third ( $P = 0.0001$ ). Mean optic nerve diameter for MOG-control mice was  $277 \pm 40 \mu\text{m}$  (mean  $\pm$  SD) relative to  $183 \pm 16 \mu\text{m}$  for MOG+ mice (Fig. 5A). Transmission electron microscopy revealed axon counts were reduced by more than two-thirds in mice with optic atrophy (Fig. 5B), relative to a MOG+ mouse that had no evidence for inflammation, demyelination, or axonal loss (Fig. 5C) and was ultrastructurally indistinguishable from MOG- mice. The optic nerves of some MOG+ mice showed few remaining axons (Fig. 5D), some with thin sheaths of myelin (Fig. 5E). In others, axons were demyelinated with hydropic and Wallerian degeneration (Fig. 5F) that leads to irreversible axonal loss.

### Apoptosis of RGCs in MOG+ Mice

Light microscopy of the retina revealed that relative to the normal nerve fiber and ganglion cell layer of control littermates without the transgene (Fig. 6A), transgenic MOG+ mice exhibited loss of retinal ganglion cells and cells with dark nuclei and shrunken cytoplasm suggestive of apoptosis (Fig. 6B). Transmission electron microscopy of the inner retina of littermates negative for the transgene revealed normal retinal ganglion cells that had large elliptical nuclei that were electron lucent along with electron lucent cytoplasm (Fig. 6C). In contrast, transgenic MOG+ mice showed RGCs with electron dense nuclei and cytoplasmic condensation (Fig. 6D). Higher magnification of an apoptotic RGC is shown adjacent to a relatively normal-appearing RGC in the MOG+ retina (Fig. 6E).

Thus, transmission electron microscopy of the retina confirmed the attrition of RGCs in MOG+ mice by apoptosis.

### Demyelination Is Absent in MOG+ Spinal Cord

While MRI excluded lesions of the brain as a source of pNF-H in serum of MOG+ mice, here we used histopathology to exclude lesions of the spinal cord as a source of increased serum pNF-H. Light microscopy of control nontransgenic littermate spinal cord revealed the central gray matter and surrounding white matter (Fig. 7A) with normal axons and myelin in the cord white matter (Fig. 7B). The spinal cords of transgenic MOG+ mice had normal appearing myelination and fiber density without lesions to suggest demyelinating inflammation or fiber loss (Figs. 7C, 7D). The absence of spinal cord lesions (Fig. 7E) in animals with axonal loss suggests that this CNS tract was not the source of elevated serum pNF-H in MOG+ mice.

### DISCUSSION

We have shown here that serum pNF-H levels are elevated in transgenic mice with isolated optic neuritis that develop visual loss, apoptosis of ganglion cells in the retina, and loss of axons in the nerve. Axonal loss is a feature of acute EAE.<sup>12</sup> Loss of RGCs is also common to chronic EAE,<sup>13,14</sup> as well as to relapsing/remitting EAE.<sup>15</sup> The incidence of optic neuritis is very high in both model systems, but so too is the incidence of myelopathy, a hallmark of EAE. Neurofilament subunits detected in the serum and cerebral spinal fluid (CSF) of EAE animals has been previously attributed to myelitis and not optic nerve degeneration.<sup>16,28</sup> Thus, the study of EAE is unsuitable for evaluations of isolated optic neuritis. Therefore, we turned to transgenic MOG+ mice that have isolated experimental optic neuritis without evidence for myelopathy clinically or histopathologically. Here we found neurofilaments were released into the systemic circulation as evidenced by their elevation in the serum of transgenic MOG+ mice and neurofilament protein levels were markedly reduced in the optic nerves of MOG+ mice. Thus, the source of elevations of neurofilament protein in serum was likely their release from damaged axons in the optic nerve. It has recently been shown that autoimmunity against a different neurofilament subunit (NF-M) can be responsible for neurodegeneration in EAE.<sup>29</sup> However, autoimmunity against NF-H or pNF-H has not been demonstrated to be a cause of axonal and RGC loss in EAE.

Axonal and neuronal loss are increasingly recognized as the primary factors contributing to persistent deficits and disability in MS and optic neuritis patients,<sup>1-4</sup> as also revealed by optical coherence tomography (OCT).<sup>30,31</sup> In multiple sclerosis, CSF pNF-H levels increased in those with primary or secondary progressive disease, but in those with relapsing remitting disease pNF-H titers were elevated acutely and decreased later.<sup>10</sup> Our results here also suggest that elevations in pNF-H reported for NMO, optic neuritis, and MS patients may be derived from damage to the optic nerve.<sup>5,8</sup> Those patient studies could not exclude damage to axons of the spinal cord or brain where MRIs may have been abnormal. In transgenic MOG+ mice using histopathology, we excluded lesions in the spinal cord that are the hallmark myelitis-causing paralysis in animals with EAE as a source of pNF-H. Still we concede that even with this model, it is not possible to be sure that serum changes are due solely to optic nerve degeneration. We know from MS patients that there can be significant axonal loss even in the absence of detectable inflammatory lesions, as many MS patients without a history of optic neuritis have RNFL thinning on OCT, and MS patients develop generalized brain atrophy

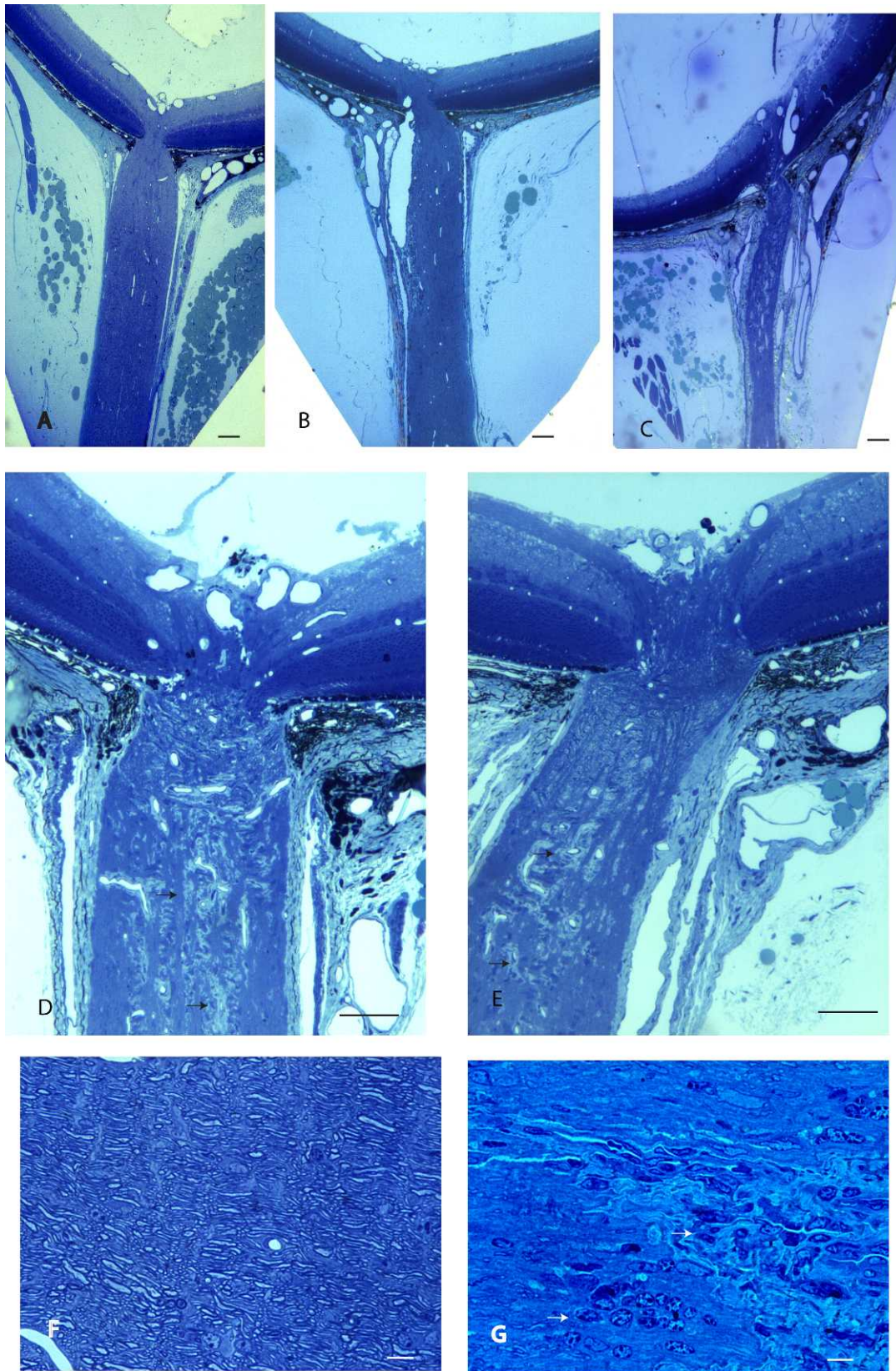


**FIGURE 4.** Optic nerve histology. Longitudinal sections of the retrobulbar optic nerve counterstained with toluidine blue show the normal retrobulbar nerve of a MOG<sup>-</sup> littermate (A), the atrophic retrobulbar optic nerve of a transgenic MOG<sup>+</sup> mouse (B), and another MOG<sup>+</sup> mouse with severe optic atrophy (C). Demyelination with loss of toluidine staining (*arrows*) is shown in the optic nerve of a transgenic MOG<sup>+</sup> mouse (D, E). At higher magnification, the optic nerve of an MOG<sup>-</sup> animal shows optic nerve fibers (F). An MOG<sup>+</sup> mouse shows inflammatory cells (*arrows*) and demyelination (G). Scale bars: 100  $\mu$ m (A-E), 10  $\mu$ m (F, G).

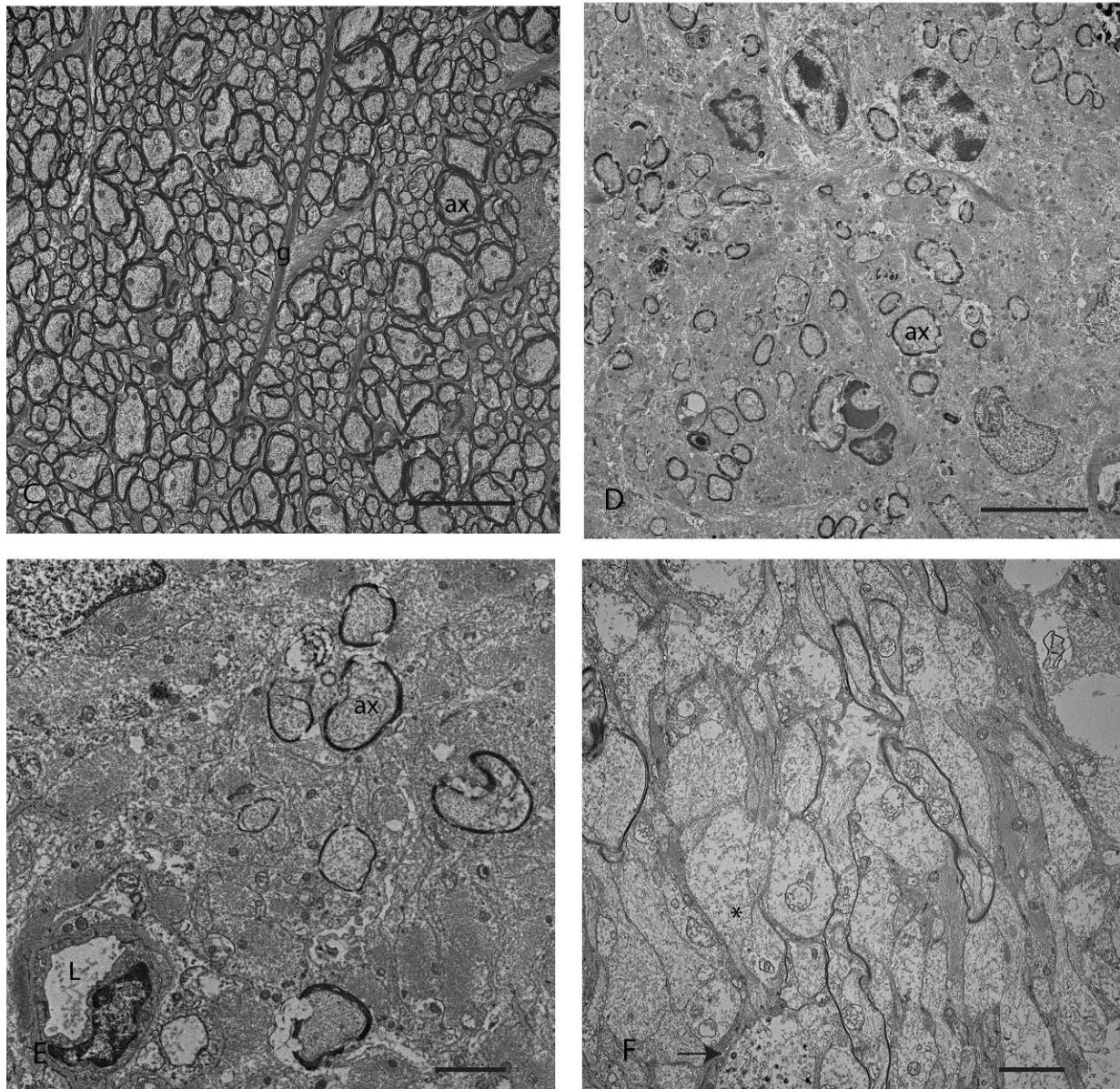
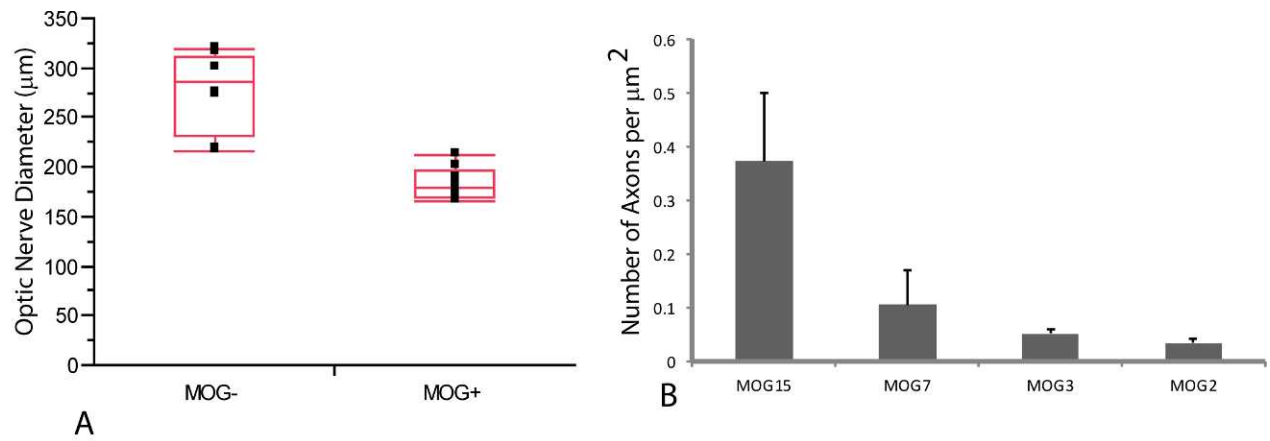


**FIGURE 5.** Optic diameter, axons counts, and transmission electron microscopy. (A) A scatterplot shows optic nerve diameters of MOG<sup>-</sup> and MOG<sup>+</sup> mice. (B) A bar plot of axon counts for four MOG<sup>+</sup> mice is shown. (C) A representative micrograph of animal MOG15 shows normal axonal density. (D) The retrobulbar optic nerve of animal MOG7 shows few axons remain, some with thin sheaths of myelin (E). (F) Many demyelinated axons with dissolution of intracellular neurofilaments (\*) and one axon with electron dense aggregations are shown (arrow). Scale bars: 10 μm (C, D), 1 μm (E, F). ax, axon; g, astroglial cell process; L, lumen.

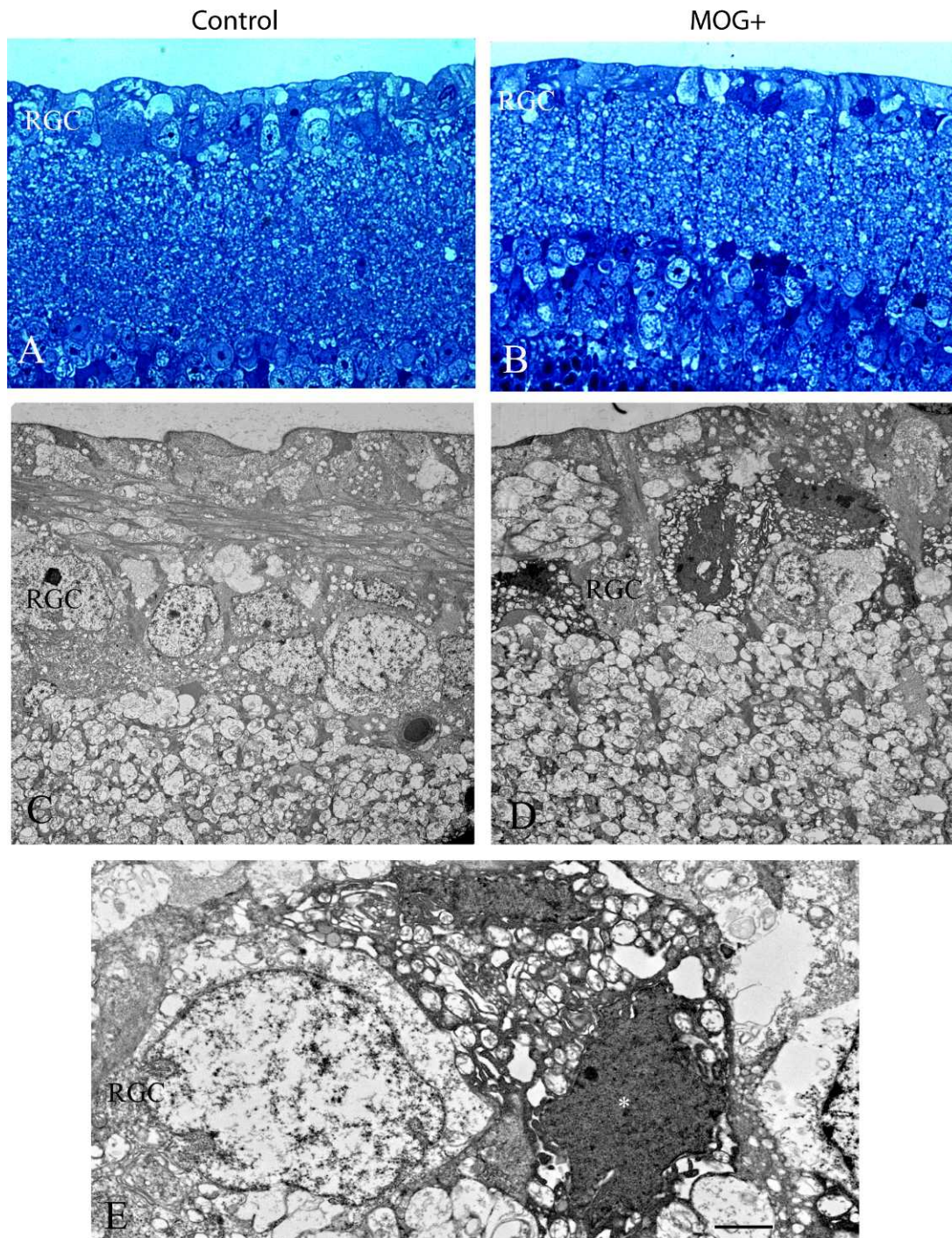


**FIGURE 6.** Apoptosis of RGCs. Light microscopy of the retina revealed that relative to the normal nerve fiber and ganglion cell layer of a control littermate without the transgene (A), a representative transgenic MOG+ mouse exhibited loss of retinal ganglion cells and RGCs with dark nuclei and condensed cytoplasm (B). Transmission electron micrographs of the inner retina of a littermate negative for the transgene revealed normal retinal ganglion cells that had large elliptical electron lucent nuclei that were surrounded by electron lucent cytoplasm (C). In contrast, the retina of a transgenic MOG+ mouse had RGCs with electron-dense nuclei and cytoplasmic condensation (D). Higher magnification of an apoptotic RGC (\*) is adjacent to a relatively normal-appearing RGC in the MOG+ retina (E). Scale bars: 2  $\mu$ m.

outside of distinct inflammatory lesions. Thus, despite the absence of visible brain MRI or histologic spinal cord lesions in MOG TCR+ mice, we could not exclude subclinical axonal injury below the resolution of the methods we used for lesion detection.

Consistent with these studies and observations, elevation of serum pNF-H has also been found in another disease that

affects primarily the optic nerve: Leber's hereditary optic neuropathy (LHON).<sup>19</sup> Petzold has demonstrated that increased levels of pNF-H can be detected in the serum of isolated optic neuritis patients<sup>6</sup> or MS patients,<sup>11</sup> and that this increase inversely correlates to their recovery of vision. The Optic Neuritis Treatment Trial patients showed an increase in serum pNF-H levels in the 5-year follow-up correlated with



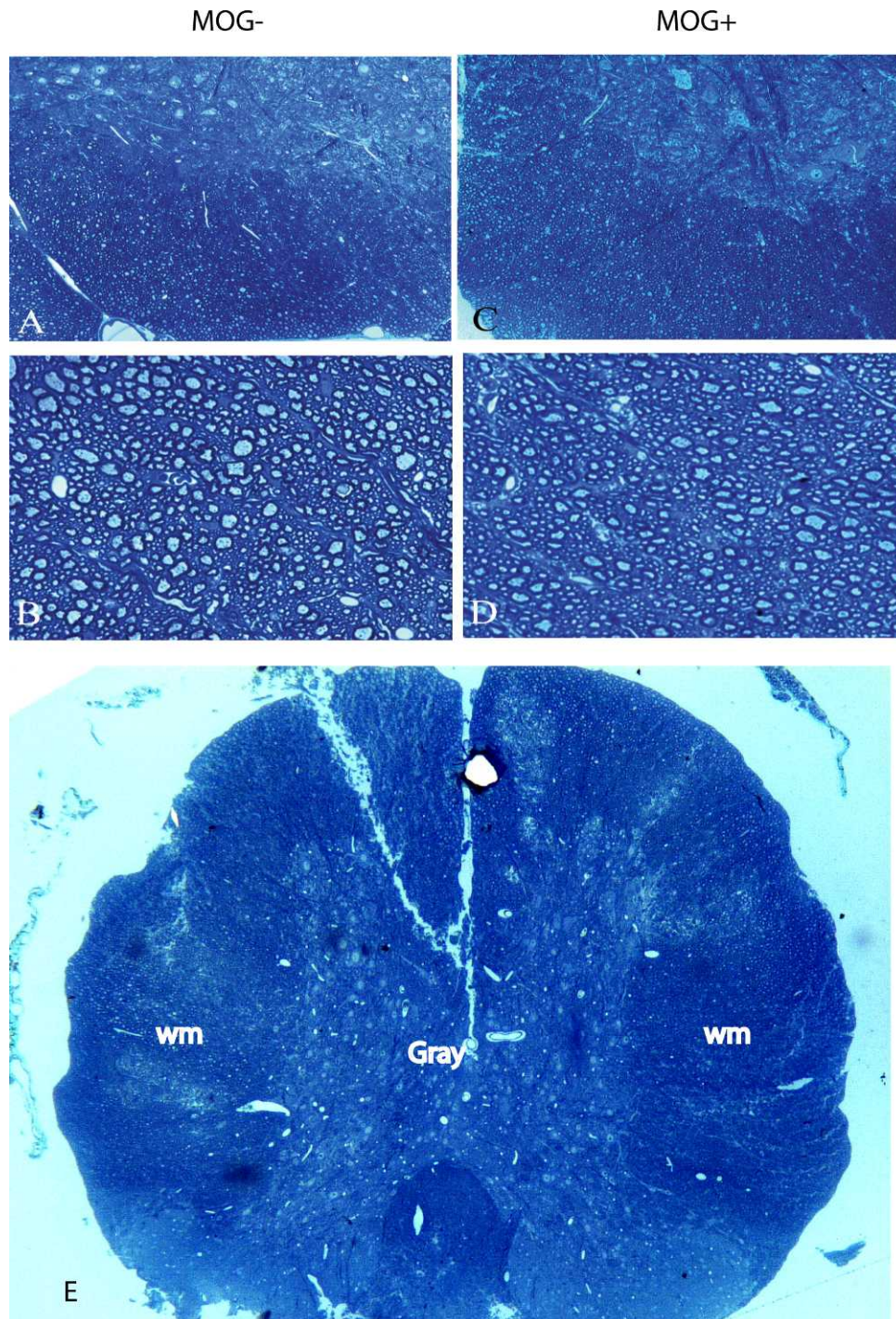


**FIGURE 7.** Histology of the spinal cord. Light microscopy of a control MOG<sup>-</sup> spinal cord shows the central gray matter and surrounding white matter (A) with normal axons and myelin in the cord white matter (B). The spinal cord of a transgenic MOG<sup>+</sup> mice had normal appearing myelination and fiber density without lesions of demyelinating inflammation or fiber loss at low (C) and high magnification (D). Low magnification of the spinal cord shows the central gray matter surrounded by the white matter (E). wm, white matter.

poorer visual function at study entry and loss of RNFL at study conclusion. Thus, serum neurofilament levels can provide a prospective measure of neurodegeneration,<sup>10</sup> as opposed to MRI or OCT measures of atrophy or thinning of the NFL that are detectable after neurons or axons have been irreversibly lost.<sup>30,31</sup>

Our results also suggest that apart from serum pNF-H levels, the PERG is also a sensitive measure of RGC dysfunction that also appears to reflect neurodegeneration in transgenic MOG<sup>+</sup>

mice. In a different transgenic mouse model (ND4), PERG amplitudes showed an early decrease compared with the neurological/gait abnormality or disability score and before demyelination.<sup>25,32</sup> Unlike the EAE and MOG<sup>+</sup> models, ND4 mice had loss of RGC dendrites but not loss of RGCs or axons. As transgenic MOG<sup>+</sup> mice rarely develop hind limb paralysis, the exact date of onset of disease is unclear. Guan and colleagues found that optic nerve neurodegeneration of MOG<sup>+</sup> mice occurred after the demyelinating inflammation.<sup>17</sup> Others

have shown early involvement of RGCs prior to the demyelinating inflammation in EAE.<sup>33,34</sup> Unlike rats with acute EAE that had swelling of the optic nerves, those of MOG+ mice with chronic optic neuritis were atrophic. Further studies on testing RGC functional deficits using the PERG and serum pNF-H levels in isolated optic neuritis and MS may give a better idea about the rate of disease progression and perhaps more importantly a method of selecting those in need of neuroprotection for treatment before irreversible neuronal and axonal loss leads to permanent disability.<sup>35,36</sup>

### Acknowledgments

We thank Mabel Wilson for editing the manuscript.

Supported by National Eye Institute (NEI) Grants R01 EY007982 (JG); EY014801 and P30EY014801 (VP); and in part from an unrestricted grant to Bascom Palmer Eye Institute from Research to Prevent Blindness, Inc.

Disclosure: **V. Talla**, None; **C. Yang**, None; **G. Shaw**, None; **V. Porciatti**, None; **R.D. Koilkonda**, None; **J. Guy**, None

### References

- Bjartmar C, Wujek JR, Trapp BD. Axonal loss in the pathology of MS: consequences for understanding the progressive phase of the disease. *J Neurol Sci*. 2003;206:165-171.
- Bjartmar C, Kinkel RP, Kidd G, et al. Axonal loss in normal-appearing white matter in a patient with acute MS. *Neurology*. 2001;57:1248-1252.
- DeLuca GC, Williams K, Evangelou N, et al. The contribution of demyelination to axonal loss in multiple sclerosis. *Brain*. 2006;129:1507-1516.
- Petzold A. Neurofilament phosphoforms: surrogate markers for axonal injury, degeneration and loss. *J Neurol Sci*. 2005; 233:183-198.
- Petzold A, Plant GT. The diagnostic and prognostic value of neurofilament heavy chain levels in immune-mediated optic neuropathies. *Mult Scler Int*. 2012;2012:217802.
- Petzold A, Rejdak K, Plant GT. Axonal degeneration and inflammation in acute optic neuritis. *J Neurol Neurosurg Psychiatry*. 2004;75:1178-1180.
- Brettschneider J, Petzold A, Junker A, et al. Axonal damage markers in the cerebrospinal fluid of patients with clinically isolated syndrome improve predicting conversion to definite multiple sclerosis. *Mult Scler*. 2006;12:143-148.
- Pasol J, Feuer W, Yang C, et al. Phosphorylated neurofilament heavy chain correlations to visual function, optical coherence tomography, and treatment. *Mult Scler Int*. 2010;2010:542691.
- Optic Neuritis Study Group. Visual function 15 years after optic neuritis: a final follow-up report from the Optic Neuritis Treatment Trial. *Ophthalmology*. 2007;115:1079-1082.
- Petzold A, Eikelenboom MJ, Keir G, et al. Axonal damage accumulates in the progressive phase of multiple sclerosis: three year follow up study. *J Neurol Neurosurg Psychiatry*. 2005;76:206-211.
- Petzold A, Brassat D, Mas P, et al. Treatment response in relation to inflammatory and axonal surrogate marker in multiple sclerosis. *Mult Scler*. 2004;10:281-283.
- Aboul-Enein F, Weiser P, Hoftberger R, et al. Transient axonal injury in the absence of demyelination: a correlate of clinical disease in acute experimental autoimmune encephalomyelitis. *Acta Neuropathol (Berl)*. 2006;111:539-547.
- Sakuma H, Kohyama K, Park IK, et al. Clinicopathological study of a myelin oligodendrocyte glycoprotein-induced demyelinating disease in LEW.1AV1 rats. *Brain*. 2004;127: 2201-2213.
- Shao H, Huang Z, Sun SL, et al. Myelin/oligodendrocyte glycoprotein-specific T-cells induce severe optic neuritis in the C57BL/6 mouse. *Invest Ophthalmol Vis Sci*. 2004;45:4060-4065.
- Raine CS, Traugott U, Nussenblatt RB, et al. Optic neuritis and chronic relapsing experimental allergic encephalomyelitis: relationship to clinical course and comparison with multiple sclerosis. *Lab Invest*. 1980;42:327-335.
- Gresle MM, Shaw G, Jarrott B, et al. Validation of a novel biomarker for acute axonal injury in experimental autoimmune encephalomyelitis. *J Neurosci Res*. 2008;86:3548-3555.
- Guan Y, Shindler KS, Tabuena P, et al. Retinal ganglion cell damage induced by spontaneous autoimmune optic neuritis in MOG-specific TCR transgenic mice. *J Neuroimmunol*. 2006; 178:40-48.
- Bettelli E, Pagany M, Weiner HL, et al. Myelin oligodendrocyte glycoprotein-specific T cell receptor transgenic mice develop spontaneous autoimmune optic neuritis. *J Exp Med*. 2003;197: 1073-1081.
- Guy J, Shaw G, Ross-Cisneros FN, et al. Phosphorylated neurofilament heavy chain is a marker of neurodegeneration in Leber hereditary optic neuropathy (LHON). *Mol Vis*. 2008;14: 2443-2450.
- Petzold A, Shaw G. Comparison of two ELISA methods for measuring levels of the phosphorylated neurofilament heavy chain. *J Immunol Methods*. 2006;319:34-40.
- Lehmensiek V, Sussmuth SD, Brettschneider J, et al. Proteome analysis of cerebrospinal fluid in Guillain-Barre syndrome (GBS). *J Neuroimmunol*. 2007;185:190-194.
- Koilkonda RD, Chou TH, Porciatti V, et al. Induction of rapid and highly efficient expression of the human ND4 complex I subunit in the mouse visual system by self-complementary adeno-associated virus. *Arch Ophthalmol*. 2010;128:876-883.
- Yu H, Koilkonda RD, Chou TH, et al. Gene delivery to mitochondria by targeting modified adeno-associated virus suppresses Leber's hereditary optic neuropathy in a mouse model. *Proc Natl Acad Sci U S A*. 2012;109:E1238-E1247.
- Porciatti V. The mouse pattern electroretinogram. *Doc Ophthalmol*. 2007;115:145-153.
- Ruggeri M, Wehbe H, Jiao S, et al. In vivo three-dimensional high-resolution imaging of rodent retina with spectral-domain optical coherence tomography. *Invest Ophthalmol Vis Sci*. 2007;48:1808-1814.
- Qi X, Lewin AS, Sun L, et al. SOD2 gene transfer protects against optic neuropathy induced by deficiency of complex I. *Ann Neurol*. 2004;56:182-191.
- Qi X, Sun L, Lewin AS, et al. Long-term suppression of neurodegeneration in chronic experimental optic neuritis: antioxidant gene therapy. *Invest Ophthalmol Vis Sci*. 2007;48: 5360-5370.
- Gnanapavan S, Grant D, Pryce G, et al. Neurofilament a biomarker of neurodegeneration in autoimmune encephalomyelitis. *Autoimmunity*. 2012;45:298-303.
- Krishnamoorthy G, Saxena A, Mars LT, et al. Myelin-specific T cells also recognize neuronal autoantigen in a transgenic mouse model of multiple sclerosis. *Nat Med*. 2009;15:626-632.
- Costello F, Coupland S, Hodge W, et al. Quantifying axonal loss after optic neuritis with optical coherence tomography. *Ann Neurol*. 2006;59:963-969.
- Trip SA, Schlottmann PG, Jones SJ, et al. Retinal nerve fiber layer axonal loss and visual dysfunction in optic neuritis. *Ann Neurol*. 2005;58:383-391.
- Enriquez-Algeciras M, Ding D, Chou TH, et al. Evaluation of a transgenic mouse model of multiple sclerosis with noninvasive methods. *Invest Ophthalmol Vis Sci*. 2011;52:2405-2411.

33. Hobom M, Storch MK, Weissert R, et al. Mechanisms and time course of neuronal degeneration in experimental autoimmune encephalomyelitis. *Brain Pathol.* 2004;14:148-157.
34. Qi X, Lewin AS, Sun L, et al. Mitochondrial protein nitration primes neurodegeneration in experimental autoimmune encephalomyelitis. *J Biol Chem.* 2006;281:31950-31962.
35. Suhs KW, Hein K, Sattler MB, et al. A randomized, double-blind, phase 2 study of erythropoietin in optic neuritis. *Ann Neurol.* 2012;72:199-210.
36. Qi X, Lewin AS, Sun L, et al. Suppression of mitochondrial oxidative stress provides long-term neuroprotection in experimental optic neuritis. *Invest Ophthalmol Vis Sci.* 2007;48:681-691.